

ESTIMATION OF THE CHLOROPHYLL CONTENTS OF TOBACCO INFECTED BY THE MOSAIC VIRUS BASED ON CANOPY HYPERSPECTRAL CHARACTERISTICS

D. Y. Xu¹, X. J. Li^{1*}, Y. Q. Dou², M. Q. Liu¹, Y. H. Yang³, J. J. Niu³

¹College of Resources and Environment, Shandong Agricultural University, Taian 271018, China; ²Tobacco Research Institute of Chinese Academy of Agricultural Sciences, Qingdao 266101, China; ³Tobacco Co. Ltd. of Linyi in Shandong, Linyi 276400, China

*Corresponding Author e-mail: lxj0911@126.com

ABSTRACT

Chlorophyll content is a very important assessment index in the growing situation of crops. Estimating the chlorophyll content of tobacco accurately is an effective means of rating tobacco disease. First, field measurements were used to obtain hyper-spectral data and the chlorophyll contents of the tobacco canopy. Then, some basic data, such as the first order derivative, vegetation index, various position variables, and the area variables, were extracted from the hyper spectrum. Then, a stepwise regression analysis is combined with the above data to establish a chlorophyll estimation model of mosaic virus-infected tobacco. The results indicate that the best chlorophyll estimation model is based on position variables and area variables. The correlation coefficient of best chlorophyll content estimation model for mosaic tobacco is 0.941 and its R^2 is 0.885. Therefore, it is considered that monitoring the chlorophyll content of mosaic-infected tobacco would be feasible with hyper-spectral technology. Furthermore, it could provide technical support for the scientific management and decision-making of the tobacco field.

Key words: hyper spectrum remote sensing, tobacco mosaic disease, chlorophyll content, regression analysis, estimation model

INTRODUCTION

It is well known that chlorophyll is a matter in leaves that absorbs light energy. Not only is it one of the essential factors for plant photosynthesis, but it is also an important physiological parameter in the process of plant growth and acts as an important indicator in the growth of plants, photosynthetic capacity, nutritional status, and so on (Jiang *et al.*, 2010). Measuring a plant's chlorophyll content is crucial for precision agriculture, in which it is important to detect crop stress and chlorosis. Furthermore, monitoring chlorophyll content can be used to detect and study plant mutations, pressure, and nutritional status (Zarco-Tejada, *et al.*, 2004). Generally, spectro- photography is used to determine chlorophyll content, and while this method accurately determines chlorophyll content, it is highly limited because it is time-consuming, and it is difficult to achieve real-time, rapid, nondestructive, and large-scale monitoring with this technology. However, hyper-spectral remote sensing technology is a real-time, rapid option. Furthermore, it can achieve rapid monitoring on the growth and nutrient status of crops without destroying the crops (Wang *et al.*, 2011). Additionally, hyper-spectral remote sensing technology has been widely used in many aspects of crop management due to its continuity, rapidity, non-destruction, and multiple bands.

Furthermore, there is a direct relationship between chlorophyll content and high spectral

reflectance. Therefore, studies on remote sensing-based chlorophyll content monitoring has been widely undertaken by numerous researchers, such as Maccioni (2001); Sims and Gamon (2002); Yang (2011); and Huang (2011). Additionally, Yang Feng used hyper-spectral remote sensing technology to study changes in the chlorophyll content and canopy spectral reflectance of wheat and rice at different growth stages (Yang *et al.*, 2010). The best vegetation index for monitoring the chlorophyll content of two kinds of crops was determined by comparing the correlation of the chlorophyll content and canopy spectral data of the above crops. Moreover, by modifying the spectral index, Yang Jie established a chlorophyll estimation model of the top leaves of rice (Yang *et al.*, 2009). Jin Linxue studied the correlation between spectral index of plants and water content of leaves and greenness value; then, they determined that the best spectral index, the best band for water content and SPAD value (Jin *et al.*, 2012). Li Minxia analyzed the relationship between the hyper-spectral characteristics and the chlorophyll content and SPAD value of apple leaves as well as studied the correlation between the SPAD value, chlorophyll content of leaves, and the differential spectra (Li *et al.*, 2010). Furthermore, Li Fangzhou conducted research on the monitoring of winter wheat chlorophyll content in irrigated and dry lands based on hyper-spectral data and achieved ideal results (Li *et al.*, 2013). In addition, there were many researchers, such as (Li *et al.*, 2008), (Peng *et al.*, 2011),

(Tang *et al.*, 2011), and so on, that established a chlorophyll content estimation model and carried out the inversion. As a result, they achieved good results. At present, many scholars have utilized hyper-spectral remote sensing to study the chlorophyll content of wheat, corn, rice, apple, and other crops, but there are few studies on inverting the chlorophyll content of tobacco with hyper-spectral technology.

The tobacco mosaic virus has a high incidence rate with a field morbidity that is usually between 5%~20%, but an individual field can reach greater than 90%. Therefore, research on the vigorous growing period of tobacco is of great importance so that the tobacco mosaic virus can be prevented and, if not entirely prevented, to at the very least be timely and efficiently controlled. In this study, hyper-spectral remote sensing technology was used to carry out a series of studies on the canopy spectra of healthy and mosaic tobacco, and the chlorophyll meter HSY-051 was used to determine chlorophyll content. Then, the correlation between the hyper-spectral information and the chlorophyll content of tobacco was analyzed, and a chlorophyll content estimation model was established in order to assess the disease grades of tobacco.

MATERIALS AND METHODS

Flow chart of methodology:

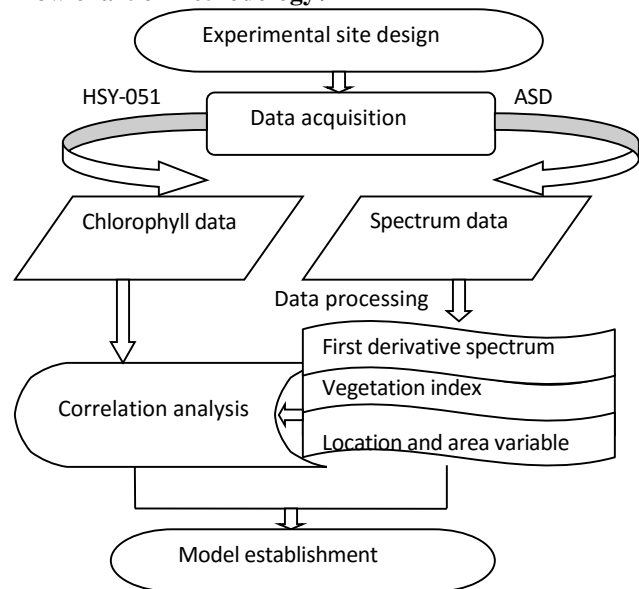


Fig.1 Technical route

Experimental site and design: The experiment was conducted in Yishui County, which is located in the north of Linyi City, Shandong Province. The site is located at 35°36' ~ 36°13' N, 118°13' ~ 119°03' E. The test area is primarily of a hilly and low mountain terrain. In this area, tobacco companies planted tobacco of the NC102 variety, and they exercise unified management over the site,

thereby ensuring unified planting and fertilization, which provided favorable conditions for smoothly implementing the test. The data was collected from June 22, 2014 to July 10, 2014, which is the vigorous growing period of tobacco. Typical plots were chosen for the test. The chlorophyll content estimation model was established based on an analysis of the hyper-spectral data, and the model was verified. For the test, six disease plots were selected, and in each plot were 50 healthy plant strains and 50 typical mosaic plant strains. The first five plots were used to establish the model, and the remaining one was used for verification.

Measurement of spectrum: Spectral reflectance was measured using a handheld spectro-radiometer (the ASD Field Spec4, ASD Company, USA). The spectral range was from 350 nm to 2500 nm. The instrument has a spectral sampling resolution of 1.4 nm and a spectral resolution of 3 nm in the 350–1000 nm range, and a spectral sampling resolution of 2 nm and a spectral resolution of 10 nm in the 1000–2500 nm range. The observation must be implemented in a cloudless and windless weather from 11:00-14:00. The sensor's probe must be vertical to the tobacco and placed 1 m away. Data was collected 3 times per tobacco plant, and the average value was calculated as the tobacco spectral. Each time, 10 sets of spectral data were taken from the tobacco. All spectral measurements must be made relative to a BaSO₄ standard reference-panel every 10 minutes to ensure the accuracy of the results.

Measurement of chlorophyll content: A large number of studies show an obvious correlation between the chlorophyll content and SPAD value, and the SPAD value could represent the change in chlorophyll content. Therefore, under certain conditions, the SPAD value determined by the chlorophyll meter can replace the direct determination of the chlorophyll content. Moreover, it is perfectly feasible to utilize the chlorophyll meter for the determination of the chlorophyll content (Yao *et al.*, 2009). In this study, the chlorophyll content was measured by the HSY-051r (unit: SPAD). For the sake of accuracy, the measurement should be taken from a piece of leaf in the upper, middle, and lower of each plant, and the measurement should be implemented twice in the top, middle, and bottom for each piece of leaf. Then, the average of the above 54 sets of data are considered to be the chlorophyll content of each tobacco plant.

Method of data processing: There will be noise in the spectrum curve due to the influence of the external environment as well as the discrepancy of different bands of spectrometer to energy response. In order to denoise the spectrum and improve the modeling accuracy, the spectral data must be smoothed, and the methods that are commonly used for smoothing are the moving average

method, polynomial fitting method, wavelet transform, and various regressions (Fang *et al.*, 2013). In this study, we elected to use the nine-point smoothing method to denoise the spectrum (He *et al.*, 2006).

After smoothing, the first derivative of the spectrum and various vegetation variables (area variable, location variable, etc.) were calculated in Excel, and the vegetation index, including the ratio vegetation index (RVI) and the normalized differential vegetation index (NDVI), were calculated in Matlab. Then, the correlation between the chlorophyll content and the mentioned variables was analyzed, and the spectrum variable of the highest correlation was screened out. Finally, the selected hyper-spectral variable was performed in order to establish the estimation model of the chlorophyll content by stepwise regression analysis in SPSS17.0. The six disease plots were divided into six groups; of which, five groups of data (250) were used to establish the model, and one group of data (50) was used for verifying the model. The parameters used in verifying the model were the coefficient of determination R^2 and the root mean square error RMSE. Excell2003, SPSS17.0, and Matlab2012 were use for data analysis and mapping.

RESULTS AND DISCUSSION

Analysis of the original spectrum and the first derivative spectrum of the tobacco mosaic:

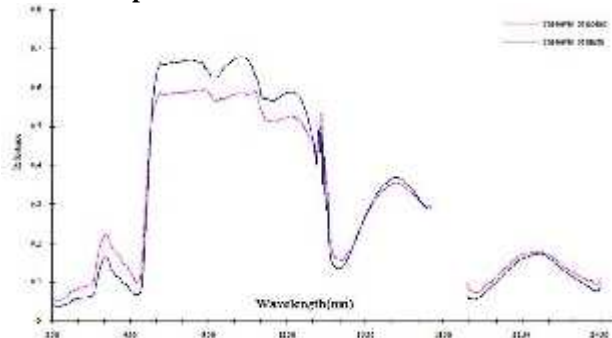


Fig. 2 Hyper-spectral curves of the original reflectance of the mosaic tobacco leaves.

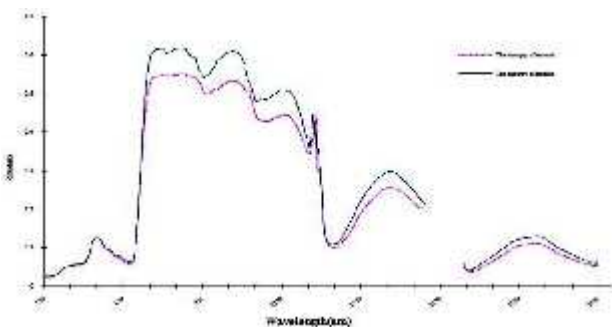


Fig. 3 Hyper-spectral curves of the original reflectance of the mosaic tobacco canopy

Figure 2 shows that the spectral reflectance of the leaves infected by the mosaic virus increases in the visible region (400-700nm) and obviously decreases in the near-infrared region (750-1300nm) because the spectral reflectance in the visible region of the vegetation leaves is primarily affected by the pigment. After being infected, the chlorophyll was destructed, both the pigment content and activity were reduced, and the color of the leaves became lighter; therefore, the spectral reflectance of the visible region increased. While in the near-infrared region, the spectral reflectance decreased because the spongy mesophyll tissue of the healthy tobacco was filled with water, which is a favorable reflector for any radiation. However, the inner structure of the tobacco changes when the plants are infected with the mosaic virus, and changes in the hindering water metabolism of the tobacco leaf tissue, chromatic agglutination, and the destruction of the structure lead to the reduction of spectral reflectance (Huang *et al.*, 1995). While the change in the canopy is less obvious than that of the leaves, the basic trend is the same, especially in the near-infrared region where the spectral reflectance of mosaic tobacco canopy is significantly lower than that of the healthy tobacco (Figure 3). The consistency of the leaves and canopy may provide a possibility for researching canopy scales.

The first derivative of the spectral reflectance for both healthy and mosaic tobacco is shown in Figure 4. The trends of the first derivative of the spectral reflectance for healthy and mosaic tobacco are generally the same. Both reach their peak at the red edge, form small reflection peaks at 520, 1000, 1220, and 1500 nm, and exhibit small reflection valleys at 930 and 1130 nm. However, the first derivative of the mosaic tobacco is obviously lower than that of the healthy tobacco. Furthermore, the green peak of the mosaic tobacco moved to the red light, and the red edge moved to the blue light.

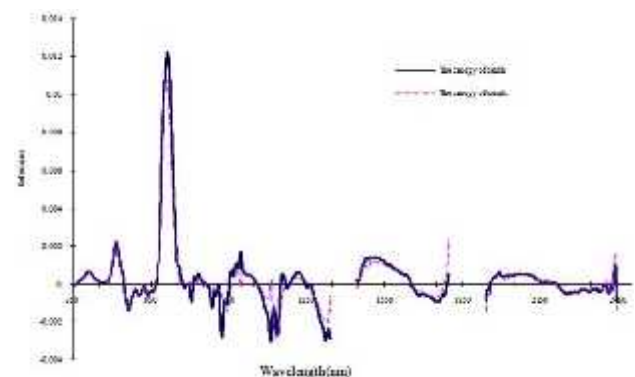


Fig. 4 First derivative hyper-spectral curves of the original reflectance of both the mosaic and healthy tobacco canopies

Analysis of the correlation between the first derivatives of the spectrum and chlorophyll content and model establishment:

There are three main methods for estimating vegetation physiological parameters using hyper-spectral remote sensing data: one is using a multiple regression method to establish a relationship between the hyper-spectral data or vegetation index and the vegetation physiological parameters (Shibayama, 1991). The second is through the red edge effect, which is effective for studying plants' conditions. More specifically, the red edge effect refers to a steep mountain ridge, known as the red edge, that occurs in the red region to the near-infrared region (660~770nm) of the vegetation reflection spectrum, and its appearance is due to the chlorophyll's influence on plant absorption (Railyan, 1993; Danso, 1995). The third is screening chlorophyll-sensitive parameters using the differential coefficient (Sun *et al.*, 2005). Here, all three of the aforementioned methods were comprehensively applied to establish the chlorophyll estimation model that is used in this study.

Analysis of the correlation between the first derivatives of the canopy and the chlorophyll content:

It can be seen from Figure 5 that there is a significant positive correlation between the chlorophyll content and

the first derivative reflectance at 663 and 717nm of the mosaic tobacco. A significant negative correlation exists between the chlorophyll content and the first derivative reflectance at 679, 1173, and 1673 nm.

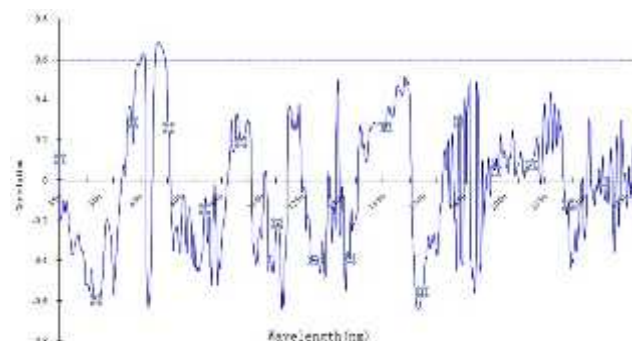


Fig. 5 Correlation analysis between the first derivative of the original reflectance of the mosaic tobacco and chlorophyll content

The chlorophyll estimation model based on the first derivative reflectance of the canopy spectrum:

The bands that had the highest correlation with the chlorophyll content were selected to establish the estimation model. The specific model can be seen in Tables 1.

Table 1 Estimation model for the chlorophyll content of mosaic tobacco based on the first derivative

Estimation model	Band combination	R	R ²
$y=19.229+1065.641 \times R'_{717}$	(717)	0.684	0.463
$y=27.450+733.315 \times R'_{717}-2041.577 \times R'_{679}$	(679,717)	0.727	0.529
$y=27.488-2922.219 \times R'_{679}-32227.005 \times R'_{1673}$	(679,1673)	0.772	0.596
$y=26.010+210.323 \times R'_{717}-2551.284 \times R'_{679}-27077.6 \times R'_{1673}$	(679,717,1673)	0.775	0.601
$y=26.524-2562.563 \times R'_{679}-22032.456 \times R'_{1673}-16782.457 \times R'_{1173}$	(679,1173,1673)	0.795	0.631

For the first derivative of the mosaic tobacco, the single band-based model had poor predictive power, and the R² value was only 0.463; the dual-band model produced a better effect was better than the single band model did, and the R² value was greater than 0.5. However, the model that was based on three bands had the best predictive power, and the R² value was over 0.6. The characteristic bands of 679, 1173, and 1673 nm are the best variables for the estimation model whose R² is 0.631 (Table 1).

Analysis of the correlation between vegetation index and chlorophyll content and model establishment:

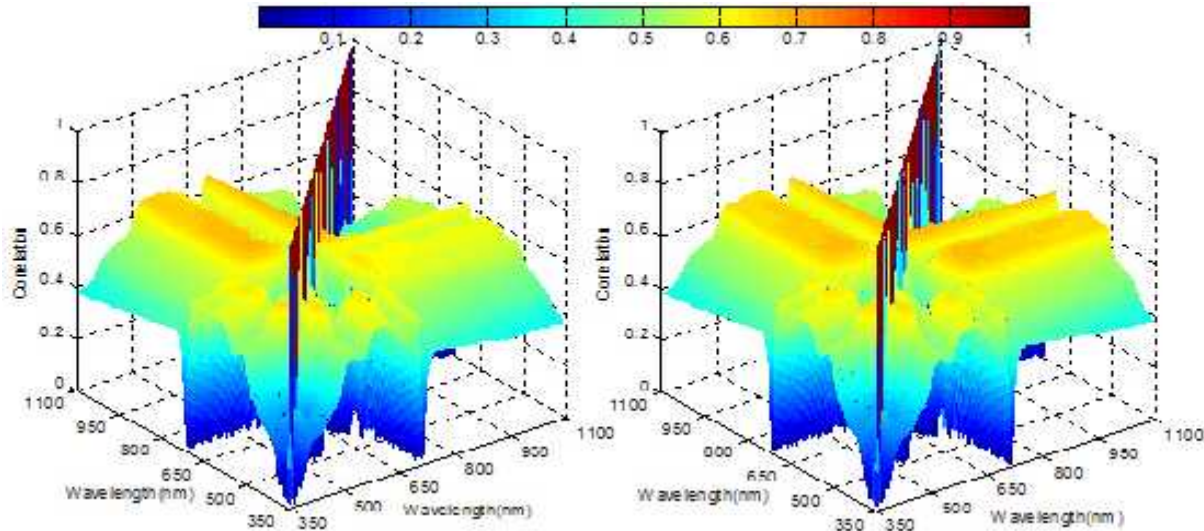
The vegetation index refers to the spectral data acquired by the remote sensor that forms into various linear and nonlinear combinations that have indicative significance for plants. As the basis of the vegetation index, RVI and NDVI are highly correlated with chlorophyll content, making it the best indicator for vegetation growth. Accordingly, RVI and NDVI were emphatically considered in this study. In order to determine the best

vegetation index, the spectral data of 350-1100nm were combined with one another, and all the vegetation indexes in this spectral range were created. The correlation diagram was completed in Matlab 2012. During plotting, the negative of the correlation was changed into positive so as to make the diagram more intuitive. The diagrams of the mosaic tobacco were shown as stereoscopic graphs (Figure 6).

The abscissa represents the numerator (350-1100nm), and the ordinate represents the denominator (350-1100nm) in the diagrams. From the chart, it can be seen that the correlation between NDVI and chlorophyll was distributed symmetrically, while RVI does not have such characteristics. The vegetation index that has the highest correlation with chlorophyll is R_{706}/R_{730} , and the correlation coefficient is 0.7004. The best NDVI is $(R_{713}-R_{712}) / (R_{713}+R_{712})$; for which, the correlation coefficient is 0.6989. The model based on RVI and NDVI is shown in Table 2.

Analysis of the correlation between location variable, area variable, and chlorophyll content and the model establishment: The correlation between the location variables, area variables, or their deformation and the

chlorophyll content was higher than that of the first derivative reflectance and vegetation index. Additionally, the correlation between the chlorophyll content and $(SDr-SDb)/(SDr+SDb)$ was greater than 0.8 (Table 3).



6(a) Correlation between RVI and chlorophyll of mosaic tobacco

6(b) Correlation between NDVI and chlorophyll of mosaic tobacco

Fig. 6 Correlation between the chlorophyll contents of the mosaic tobacco and their RVI and NDVI

Table 2. Vegetation index and its correlation with chlorophyll

Vegetation variables	Band combination	Estimation model	R ²
RVI=Rn/Rm	R ₇₀₆ /R ₇₃₀	y=52.384-41.640x	0.491
NDVI=(Rn-Rm)/(Rn+Rm)	(R ₇₁₃ -R ₇₁₂)/(R ₇₁₃ +R ₇₁₂)	y=952.159x+14.334	0.489

Table3. Locator variables, area variables, and vegetation variables and their correlation with chlorophyll

Variables	Meanings	R
r	The wavelength corresponding to the amplitude of the red edge	0.797767
Dr	The biggest first derivative reflectance of 680-760nm	0.499276
b	The wavelength corresponding to the amplitude of the blue edge	0.680196
Db	The biggest first derivative reflectance of 490-530nm	-0.34167
y	The wavelength corresponding to the amplitude of the yellow edge	0.645021
Dy	The biggest first derivative reflectance of 560-640nm	0.165184
g	The wavelength corresponding to the green peak	-0.50023
Rg	The biggest reflectance of 510-560nm	-0.46210
v	The wavelength corresponding to the red valley	-0.55415
Rr	The smallest reflectance of 640-680nm	-0.45855
SDr	The area surrounded by the first derivative reflectance of the red edge	0.708926
SDb	The area surrounded by the first derivative reflectance of the blue edge	-0.49617
SDy	The area surrounded by the first derivative reflectance of the yellow edge	0.124653
Rg/Rr	The ratio of the green peak and red valley	0.21492
(Rg-Rr)/(Rg+Rr)	The normalized value of the green peak and red valley	0.198238
SDr/SDb	The ratio of the red edge's area and blue edge's area	0.714908
SDr/SDy	The ratio of the red edge's area and yellow edge's area	-0.63832
(SDr-SDb)/(SDr+SDb)	The normalized value of the red edge's area and blue edge's area	0.832503
(SDr-SDy)/(SDr+SDy)	The normalized value of the red edge's area and yellow edge's area	-0.78898

Table 4. Estimation model for the chlorophyll content of mosaic tobacco based on each variable

Estimation model	R	R ²
$y=2.718+41.791\frac{SDr-SDb}{SDr+SDb}$	0.833	0.693
$y=-12.584+53.796\frac{SLR-SLb}{SDr+SDb}+34.328Rg$	0.861	0.742
$y=-23.030+81.794\frac{SDr-SDb}{SDr+SDb}+33.402Rg-1.452\frac{SDr}{SDb}$	0.884	0.782
$y=17.616+72.105\frac{SDr-SDb}{SDr+SDb}+40.515Rg-2.132\frac{SDr}{SDb}-23.006\frac{SDr-SDy}{SDr+SDy}$	0.917	0.841
$y=109.658+21.208\frac{SDr}{SDr+SDb}+115.622Rg-2.230\frac{SLR}{SLb}-65.138\frac{SDr-SDy}{SDr+SDy}-161.06 r$	0.941	0.885

The chlorophyll content estimation models of mosaic tobacco were established by stepwise regression. The specific models are shown in Tables 4. The chlorophyll content estimation models based on location variables, area variables, and their deformation had better predictive power than that of the first derivative reflectance and vegetation index. Furthermore, all of the R² value of the above five models were greater than 0.69.

Model testing: The accuracy of the model is primarily verified by the correlation coefficient R and the Root Mean Square Error Predict (RMSEP). The formula of RMSEP is:

$$RMSEP = \sqrt{\frac{\sum_{i=1}^n (Y_i - y_i)^2}{n}} \quad (1)$$

Y_i represents the estimated value, and y_i represents the measured value.

The R value of the model was 0.941, and its RMSEP was 1.4076. The results showed the perfect prediction of the model and that it could predict the chlorophyll content of tobacco.

For further testing, the 50 sets of data from the sixth plot were used to determine and create the 1:1 correlation graph of the estimated value and the measured value of the chlorophyll content.

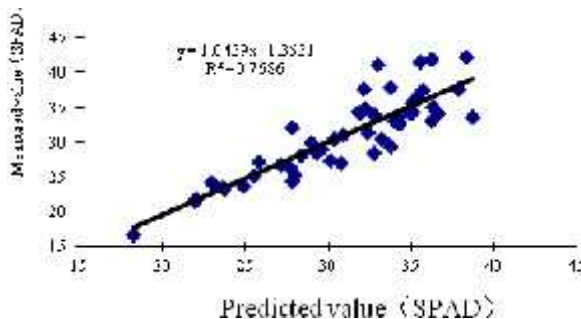


Fig.7 Validation result of the chlorophyll content estimation model of mosaic tobacco

The chlorophyll content estimation model of the mosaic tobacco was effective, and its R² was 0.7686 (Fig.7). Furthermore, this demonstrates that the model estimates well the chlorophyll content of tobacco mosaic.

Conclusions: The chlorophyll content estimation model was established by a field-measured value based on hyper-spectral and HSY-051. The accuracy of the model was high and was close to field conditions. Thus, the model could assess the chlorophyll content of mosaic tobacco. Furthermore, the method possesses certain advantages in practical application.

There were certain rules about the canopy of mosaic virus-infected tobacco through the comparison of the original spectral reflectance of mosaic tobacco with that of healthy tobacco. One of the most notable rules was that the spectral reflectance of mosaic tobacco increases in the visible region (400-700nm) and obviously decreases in the near-infrared region (700-1300nm). And as for mosaic tobacco, the green peak moved to the red region and the red edge moved to blue region. These rules provided possibilities for the follow-up work.

The chlorophyll content estimation models of mosaic tobacco were established by the regression analysis of the chlorophyll content and the reflectance of mosaic tobacco. The best model was established by (SDr-SDb)/ (SDr+SDb), Rg, SDr/SDb, (SDr-SDy)/ (SDr+SDy), and r with an R² of 0.885. This indicates that the chlorophyll content estimation model established by the stepwise regression method can predict the chlorophyll content of tobacco well.

REFERENCES

Danso, F. M. (1995). Red edge response to leaf area index. *Int. Remote Sens.* 16(1):183-188.
 Fang, X. Y., X. C. Zhu, L. Wang, and G. X. Zhao (2013). Hyperspectral monitoring of the canopy chlorophyll content at apple tree prosperous fruit stage. *Sci. Agr. Sin.* 4(16):3504-3513.

- He, T., J. Wang, and Y. Cheng (2006). Spectral features of soil moisture. *Acta Pedologica Sin.* 43 (6):1027-1032.
- Huang, J. F. and G. A. Blackburn (2011). Optimizing predictive models for leaf chlorophyll concentration based on continuous wavelet analysis of hyperspectral data. *Int. J. Remote Sens.* 32(24): 9375-9396.
- Huang, Z. X., H. Li and W. J. Chen (1995). On the observation of ultrastructure of tobacco leaf cells infected by tobacco mosaic virus. *J. Yunnan Normal Univ.* 15(2):58-67.
- Jiang, J.B., Y.H. Chen and W.J. Huang (2010). Using hyperspectral remote sensing to estimate canopy chlorophyll density of wheat under yellow rust stress. *Spectrosc. Spect. Anal.* 30(8):2243-2247.
- Jin, L. X., Y.X. Li, and D.F. Xu (2012). Spectroscopy diagnostics of water content and greenness features in wheat leaf. *Chinese J. Agrometeorol.* 33(1):124-128.
- Li, F. X., B. Zhang and D. W. Liu (2008). Hyperspectral remote sensing estimation models for chlorophyll a concentration of *calamagrostis angustifolia*. *J. Hydroecol.* 27 (7): 1077-1083.
- Li, F. Z., M. C. Feng, and W. D. Yang (2013). Monitoring of winter wheat chlorophyll content in irrigated and dry lands of Shanxi Province of China based on hyperspectral remote sensing. *J. Hydroecol.* 32(12):3213-3218.
- Li, M. X., L. S. Zhang and B. Z. Li (2010). Relationship between spectral reflectance feature and their chlorophyll concentrations and SPAD value of apple leaves. *J. Northwest Forest. Univ.* 25(2):35-39.
- Maccioni, A., G. Agati and P. Mazzinghi (2001). New vegetation indices for remote measurement of chlorophylls based on leaf directional reflectance spectra. *J. Photoch. Photobio.* 61(1/2): 52-61.
- Peng, Y. K., H. Huang and W. Wang (2011). Rapid detection of chlorophyll content in corn leaves by using least squares-support vector machines and hyperspectral images. *J. Jiangsu Univ.* 32(2): 125-128.
- Railyan, V. Y. (1993). Red edge structure of canopy reflectance spectra of triticale. *Remote Sens. Environ.* 46(2):173-182
- Shibayama (1991). Estimating grain yield of maturing rice canopies using high spectral resolution reflectance measurements. *Remote Sens. Environ.* 36(1):45-53.
- Sims, D. A. and J. A. Gamon (2002). Relationships between leaf pigment content and spectral reflectance across a wide range of species, leaf structures and developmental stages. *Remote Sens. Environ.* 81(2): 337-354.
- Sun, X. M., Q. F. Zhou and Q. X. He (2005). Hyperspectral variables in predicting leaf chlorophyll content and grain protein content in rice. *Acta agron. Sin.* 31(7):844-850.
- Tang, X. G., K. S. Song and D. W. Liu (2011). Comparison of method for estimating soybean chlorophyll content based on visual/near infrared reflection spectra. *Spectrosc. Spect. Anal.* 31(2): 371-374.
- Wang, K. R., W. C. Pan and S. K. Li (2011). Monitoring models of the plant nitrogen content based on cotton canopy hyperspectral reflectance. *Spectrosc. Spect. Anal.* 31(7):1868-1872.
- Yang, F., Y. M. Fan and J. L. Li (2010). Estimating LAI and CCD of rice and wheat using hyperspectral remote sensing data. *Trans. of the CSAE.* 26(2):237-243.
- Yang, J., Y. C. Tian and X. Yao (2009). Hyperspectral estimation model for chlorophyll concentrations in top leaves of rice. *Acta Ecol. Sin.* 29(12): 6561-6571.
- Yang, X. H., J. F. Huang and Y. P. Wu (2011). Estimating biophysical parameters of rice with remote sensing data using support vector machines. *Sci. China (Life Science)*, 54(3): 272-281.
- Yao, F. Q., Z. H. Zhang and Y. R. Yang (2009). Hyperspectral models for estimating vegetation chlorophyll content based on red edge parameter. *Trans. of the CSAE.* 25(2):123-129.
- Zarco-Tejada, P. J., J. R. Miller and A. Morales (2004). Hyperspectral indices and model simulation for chlorophyll estimation in open-canopy tree crops. *Remote Sens. Environ.* 90:463-476.